

OPEN ACCESS

Review—Two-Dimensional Titanium Carbide MXenes and Their Emerging Applications as Electrochemical Sensors

To cite this article: Tian Yu and Carmel B. Breslin 2020 *J. Electrochem. Soc.* **167** 037514

View the [article online](#) for updates and enhancements.

EXTENDED ABSTRACT DEADLINE: DECEMBER 18, 2020



239th ECS Meeting

with the 18th International Meeting on Chemical Sensors (IMCS)



May 30-June 3, 2021

SUBMIT NOW →



Review—Two-Dimensional Titanium Carbide MXenes and Their Emerging Applications as Electrochemical Sensors

Tian Yu and Carmel B. Breslin *,^z

Department of Chemistry, Maynooth University, Maynooth, Co. Kildare, Ireland

MXenes, new two-dimensional transition metal carbides and nitrides, are attracting considerable attention as multifunctional materials in various research fields due to their high surface area, hydrophilicity, good mechanical properties, metallic-like conduction and adsorption characteristics, combined with the ability to tailor the surface properties with functional groups. In this review, the applications of MXenes as electrochemical sensors are summarised and discussed. The review is focused on $Ti_3C_2T_x$ as these are the only MXenes that have so far been considered as electrochemical sensors, primarily due to the fact that they have metallic-like conduction and can be easily formed as single and multi-layered flakes through chemical etching of the parent MAX phase. The fabrication of the $Ti_3C_2T_x$ -based sensors is first described and then followed by an account of their applications as electrochemical sensors, for the detection of small molecules, environmental contaminants and biosensors for biomedical sensing applications. Finally, their overall stability when exposed to aqueous media, which will have implications in the future development of MXene-based sensors, is discussed together with their future prospects as electrochemical-based sensors.

© The Author(s) 2019. Published by ECS. This is an open access article distributed under the terms of the Creative Commons Attribution 4.0 License (CC BY, <http://creativecommons.org/licenses/by/4.0/>), which permits unrestricted reuse of the work in any medium, provided the original work is properly cited. [DOI: 10.1149/2.0142003JES]



Manuscript submitted September 16, 2019; revised manuscript received November 4, 2019. Published December 9, 2019. *This paper is part of the JES Focus Issue on Sensor Reviews.*

Since their discovery in 2011,¹ MXenes have attracted considerable interest and attention and have been described in several reports as the ‘shining star’ in renewable energy and indeed in other applications. They have been considered for applications in several different areas, such as electrochemical energy storage,² including lithium ion batteries,^{3,4} environmental remediation,^{5,6} as capacitors,^{7,8} as photocatalysts for water splitting,⁹ electro- and photocatalysis,¹⁰ in biomedical applications^{11,12} and more recently they have emerged as novel materials in the design and fabrication of electrochemical sensors.^{11–14}

MXenes are a family of two dimensional metal carbides or nitrides, which are derived from their corresponding parent and 3-dimensional layered MAX phase.¹⁵ The MAX phases are represented as $M_{n+1}AX_n$, where M is an early transition element, such as Ti, A represents a Group 13 or 14 element, with Al being the most popular, while X is carbon or nitrogen and n represents an integer, with $n = 1, 2$ or 3 . The MAX phases are stacked in a hexagonal lattice, separated by A atoms. The MXenes are formed by selectively etching the A element as the bonding between M-A is generally weaker than M-X (for $Ti_{n+1}AlC_n$)^{16,17} to give $M_{n+1}X_nT_x$, where T_x represents the terminal groups introduced during the selective dissolution of the A element.¹⁵ The M-X bonds are considered to be strong and similar to their binary MX counterparts,^{16,17} so that the M and X elements are retained during the etching process. Depending on the experimental conditions employed in etching, such as the etchant, temperature and time, T_x may represent $-F, -Cl, -O$ or $-OH$ terminal groups.^{1,15} This etching step is then followed by an exfoliation step to give colloidal suspensions of single or a few layers of MXenes.^{15,18} It is also possible to use liquid exfoliation by selecting molecules that have the capacity to weaken the inter-layer interactions in the MXenes layers.¹⁹ This is normally achieved as the molecules are intercalated and induce swelling of the interlayer space and this method can be employed to convert the multilayers into single nanoflakes, with a high yield of the 2-dimensional flakes. Using this top-down synthetic approach a variety of different MXenes have been formed including, $Ti_3C_2T_x, Ti_2CT_x, Mo_2CT_x, Ti_4N_3T_x, Nb_2CT_x$ and $Zr_3C_2T_x$.^{20,21} Double transition metal MXenes such as $Mo_2TiC_2T_x$ and $Mo_2Ti_2C_3T_x$ have also been formed.^{22,23} Until recently, Al was the only element that could be etched from the parent MAX phase, but recently it was shown that Si could be selectively removed from $Ti_3Si_2C_2$ using HF and H_2O_2 .²⁴

In terms of electrochemical sensors, MXenes have a number of attractive properties and more importantly, the properties can be further tailored through the selection of the M and X elements and the

surface termination groups. It has been shown that the M layer has a significant influence on the electronic properties, with metallic-like conduction being observed for Ti_3C_2 , while Mo_2TiC_2 exhibits semi-conducting properties.^{25,26} The terminal surface groups can also influence not only the electrochemical performance, but also electronic and optical properties of the MXenes.^{27,28} The terminal groups can be altered to some degree using thermal treatments, with $-OH$ and $-F$ groups being transformed into $-O$ groups, while $-OH$ groups can be introduced by treating the MXenes in NaOH solutions, an alkylation or hydroxylated process.²⁹ In addition to good conductivity and interesting surface chemistries, MXenes have the potential to be employed for further surface modification with functional groups. MXenes, like carbon nanotubes (CNTs) and graphene layers, have a high surface area with good mechanical properties, but they also exhibit hydrophilicity compared to the more hydrophobic graphene and CNTs. In recent reports they have been described as having good biocompatibility.³⁰ The titanium carbides, $Ti_3C_2T_x$ and Ti_2CT_x , are the most extensively studied with the $Ti_3C_2T_x$ being considered to have excellent conducting properties, with the conductivity reaching 4600 S cm^{-1} .^{31,32} These are the MXenes that have been considered in most electrochemistry applications and particularly in the fabrication of electrochemical sensors.

In this paper, recent advances in the application of MXenes as electrochemical-based sensors are summarised, with a focus on the electrochemical detection of small molecules, environmental contaminants and biosensors. Finally, the challenges and future opportunities and prospects of MXenes in the design of electrochemical sensors are discussed. A number of excellent reviews is already available that describe the current status and recent progress on the synthesis of MXenes,^{15,20,33,34} their biomedical applications,^{11,12} adsorptive remediation of water and air pollutants,³⁵ environmental applications^{36–38} the electrocatalytic properties of MXenes,^{39,40} while Sinha et al.¹⁴ have reviewed recent advances in sensors, including solid state gas, piezoresistive and photoluminescent sensors. Therefore, this review is focused on the preparation of MXenes, their applications as electrochemical sensors and biosensors and their overall stability when exposed to aqueous media, which will have implications in the future development of MXene-based sensors.

MXenes as Electrochemical Sensors

As detailed earlier, MXenes are emerging as an interesting and exciting material for electrochemical sensors, with very good conducting properties, high surface area, arising from the two-dimensional structure, and they can be easily modified with metal nanoparticles and incorporated with other materials to give composite sensors. Compared

*Electrochemical Society Member.

^zE-mail: Carmel.Breslin@mu.ie

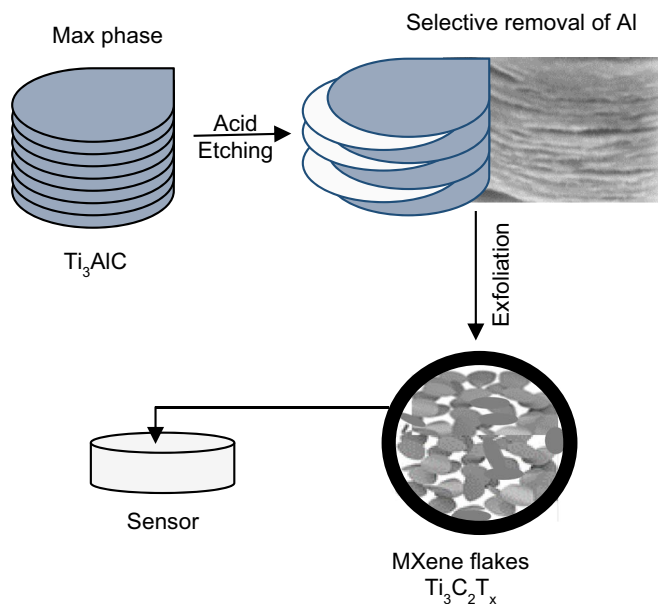
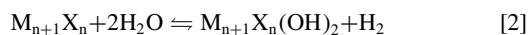
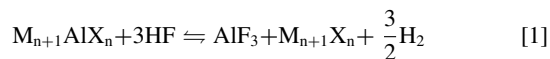


Figure 1. Schematic illustrating the formation of 2-dimensional MXene flakes from the initial MAX phase starting material.

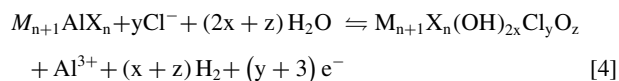
to two-dimensional graphene,^{41–43} they are much less well known as electrochemical sensors. However, unlike graphene, which is highly hydrophobic,⁴⁴ MXenes have very good hydrophilicity. The recent applications of MXenes as electrochemical sensors are described following a short summary of the procedures used in the fabrication of MXene-based sensors.

Etching and fabrication of MXene electrodes and sensors.—MXenes are formed by the selective etching of the A layer from the parent MAX phase, as illustrated in the schematic in Figure 1. The MAX parent phases are comprised of a family of approximately 130 different compositions. However, most of them adopt the $P6_3/mmc$ space group, consisting of MX_6 octahedra which are interleaved with the group A element layers.^{1,17,32} In order to dissolve and etch the A layers, aggressive and acidic conditions are required and HF is normally employed.^{10,13,20} The acid etching process can be summarised in Equations 1 to 3 where A is Al to give MXenes with $-F$ and $-OH$ terminal groups.



Typically, a 50 wt% solution of HF with a 2-h etching period is employed in the etching of Ti_3AlC_2 .¹ As illustrated in Equation 1, the Al atoms are removed from between the layers to give $M_{n+1}X_n$ and the resulting Al^{3+} is released into the solution phase. The exposed Ti atoms are satisfied by either fluoride, Equation 3, or hydroxyl anions, Equation 2.¹ However, due to the high toxicity of HF, various attempts have been made to modify the etching process and reduce or eliminate the need for HF and these developments are all relevant to the fabrication of MXene-based electrochemical sensors, as the nature of defects and the functional groups are important in initial adsorption and/or the charge-transfer step. One of the earliest methods, described as the in-situ generation of HF, employed fluoride salts, NaF, KF, LiF and FeF_3 , together with HCl.⁴⁵ Again, highly acidic conditions are generated with high concentrations of salts and acids, one example being 1.9 M LiF and 6 M HCl.⁴⁶ It was also concluded that intercalation of the cations (Li^+ , K^+ , Na^+) into the interlayered spaces weakened the interlayer interactions facilitating exfoliation. The addition of HCl to the etching solution also gives rise to $-Cl$ terminal

groups. Although the presence of the H^+ and F^- in the solution phase gives rise to HF, this medium is less aggressive, and was shown to give rise to high exfoliation yields with approximately 70% of the flakes being of one or two layers, and a lower amount of defects. Electrochemical etching has also been proposed and demonstrated. For example, Sun et al.⁴⁷ confirmed that Ti_2AlC can be electrochemically etched in low concentrations of HCl to give a three-layered structure, with carbides (where both the Ti and Al was etched), MXene and the un-etched MAX phase. The MXenes were further separated from this three-layer structure and etching of the A phase was described by Equation 4. In a later study, Pang et al.⁴⁸ achieved the selective removal of Al by employing a thermal-assisted electrochemical etching strategy, where a composite electrode involving the MAX phase, Ti_2AlC , carbon black (CB) and carbon fiber cloth (CFC) was employed. The porous CFC and the highly conductive CB were used to give more efficient electrochemical reactions and higher currents. The selective etching of Al was achieved at 0.3 V vs RHE without the oxidation of Ti in a dilute HCl solution at 50°C, as described in Equation 4. Feng and co-workers,⁴⁹ also achieved the selective electrochemical oxidation of Al from Ti_3AlC_2 in an alkaline pH 9.0 electrolyte with ammonium chloride (NH_4Cl) and tetramethylammonium hydroxide ($N(CH_3)_4OH$).



The various etching solution reagents and techniques are summarised in Table I, where it is clear, and not surprising, that the surface terminal groups depend on the composition of the etching solution. However, the etching conditions employed also influence the defect structure. It has been shown that higher defect concentrations are formed on increasing the HF concentration.⁴⁶ Atomic scale defects arise due to the formation of vacancies in the Ti sublayers and these are formed when the surface Ti atoms are etched and removed by the acid. For example, Sang et al.⁴⁶ have shown that vacancies are rarely observed with a 2.7 wt% HF concentration, but are readily seen with the more acidic 7 wt% HF solution. It was shown that less defective MXenes are formed with shorter etching times, but the rate of conversion from the MAX phase to the MXene is lower.⁶ Currently, it is not possible to generate terminal group free MXenes with no defects using this top-down synthesis approach. However, it was concluded, using Density Function Theory (DFT) calculations, that $-OH$ terminated Ti_3C_2 should exhibit high conductivity even with moderate concentrations of defects.⁴⁶

Typically, this etching step is followed by some exfoliation process, either sonication, shaking or liquid exfoliation, and the acid is removed by washing with copious amounts of distilled or deionised water. This is continued until a pH of about 6.0 or 7.0 is reached, signifying the complete removal of the acid. The resulting $M_{n+1}X_nT_m$ flakes are best stored as powders as MXenes undergo oxidation or hydrolysis reactions as colloidal solutions and this ultimately converts them into titania in aqueous media.^{50–52} Alternatively, they can be maintained as stable inks in solvents such as N-methyl-2-pyrrolidone (NMP) under an inert atmosphere.⁵² MXene-based electrodes or sensors can be fabricated using a number of methods, including the formation of paste electrodes, where the MXene is combined with an oil to form a MXene modified carbon paste electrode,^{53,54} which is very similar to that employed with other carbon-based materials.^{55,56} Drop casting, which is frequently used with carbon nanotubes⁵⁷ and graphene,^{58,59} is the most commonly employed method where the MXene is dispersed in an organic solvent and then drop cast onto a previously prepared surface.^{60–62} Also, inkjet printing onto metal foils or paper has been achieved with MXenes.⁶³ A number of other processes has been used to create conducting MXene films and these approaches could also be used to form MXene-based sensors. For example, Taylor and co-workers⁶⁴ employed a spin-casting method to give $Ti_3C_2T_x$ films with an electronic conductivity of $3092 S cm^{-1}$. MXenes can also be combined with conducting polymers,⁶⁵ metal

Table I. Summary of some etching conditions employed and the resulting functional terminal groups.

Reagents/technique	MXenes	Surface groups	Ref.
HF	$M_{n+1}X_nT_m$ (nearly all)	-F-OH	10,13,20
In-situ HF (fluoride salts and HCl)	$Ti_3C_2T_m$	-F, -OH-O, -Cl	45
Electrochemical/ $NH_4Cl/TMAOH$	$Ti_3C_2T_m$	-OH, -O	49
Electrochemical/HCl	$Ti_3C_2T_m$	-OH, -Cl, -O	47,48

nanoparticles,^{66,67} graphene^{68,69} and carbon nanotubes⁷⁰ to give highly conducting substrates.

MXene sensors for small molecules.—There is considerable interest in the electrochemical detection of small molecules, including H_2O_2 , dopamine (DA), epinephrine (EP), ascorbic acid (AA), uric acid (UA) and acetaminophen (APAP).^{71–73} The detection and quantification of H_2O_2 is important in the pharmaceutical, food, clinical and environmental sectors. It also plays an important role in natural oxidation processes, while it is one of the most important substrates of enzyme-catalysed oxidation reactions. AA, more commonly known as vitamin C, is an essential nutrient, while DA is an important neurotransmitter. APAP, also known as paracetamol, is extensively used in the treatment of fever, while changes in the concentration of UA have been linked with several diseases, such as renal failure. Moreover, the selective detection of UA, DA and AA is important as these molecules co-exist with a large excess of AA, making the electrochemical detection of UA and DA in the presence of AA difficult.

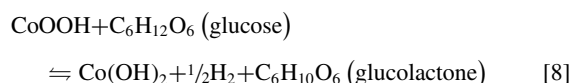
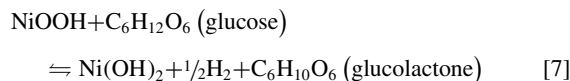
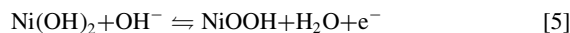
These molecules have all been detected using MXene-based electrochemical sensors. Using $Ti_3C_2T_x$, a highly sensitive H_2O_2 sensor was formed.⁷⁴ However, it was susceptible to anodic oxidation once the applied potential was increased to values higher than 430 mV vs Ag|AgCl. In a later study, the same group modified the $Ti_3C_2T_x$ with platinum nanoparticles ($Ti_3C_2T_x/PtNp$) to give enhanced stability.⁷⁵ Not only did the presence of the platinum nanoparticles provide stability, but the reduction of H_2O_2 was achieved at higher potentials. At an applied potential of 0.0 V vs Ag|AgCl, the limit of detection was measured as 883 $\mu M H_2O_2$ for the $Ti_3C_2T_x$ while it was lowered to 0.448 $\mu M H_2O_2$ when the platinum nanoparticles were combined with the MXene, illustrating the advantage of combining metal nanoparticles and MXenes. Zheng et al.⁷⁶ fabricated an inkjet-printed H_2O_2 sensor using a $Ti_3C_2T_x$ graphene oxide nanocomposite. The graphene oxide was used to enhance the stability of the $Ti_3C_2T_x$ slurry. A dynamic linear range between 2.0 μM and 1.0 mM with a detection limit of 1.95 $\mu M H_2O_2$ was obtained. These studies indicate that the stability of the $Ti_3C_2T_x$ nanoflakes can be enhanced by forming composites with metal nanoparticles or graphene.

The platinum nanoparticle modified $Ti_3C_2T_x$ was also employed in the detection of APAP, DA, AA and UA with detection limits of 0.13 μM , 0.26 μM , 0.25 μM and 0.12 μM , respectively.⁷⁵ Using differential pulse voltammetry, it was possible to distinguish between the oxidation waves of APAP and UA, but overlapping waves were seen with AA and DA. Using Nafion as a membrane, which is well known to expel anionic species,^{77,78} such as AA at near neutral pH values, the selective detection of DA in the presence of AA was possible. However, these studies were carried out with equal concentrations of AA, APAP, DA and UA (0.76 mM) whereas AA concentrations are typically much higher than DA. Shahzad et al.⁷⁹ also observed the selective sensing of DA using Nafion-stabilised $Ti_3C_2T_x$ MXenes, and concluded that the negatively charged MXene surface facilitated its detection.

Zheng et al.⁸⁰ prepared a highly sensitive and selective DA sensor by using DNA adsorbed onto $Ti_3C_2T_x$ to induce the in-situ growth of palladium nanoparticles (PdNp), with subsequent reduction of platinum to give platinum nanoparticles (PtNp). The resulting $Ti_3C_2T_x/DNA/PdNp/PtNp$ composite displayed a rapid current response, very good selectivity in the presence of AA, UA and glucose with a linear DA concentration range of 0.2 to 1000 μM and a limit of detection of 30 nM for DA. The oxidation potential for DA

was observed at about 150 mV vs Ag|AgCl somewhat lower than that observed by Lorencova et al.⁷⁵ for $Ti_3C_2T_x/PtNp$, at approximately 300 mV vs Ag|AgCl. This suggests that the selective detection of DA in the presence of excess AA can be achieved without a permselective membrane, by lowering the oxidation potential of DA and this appears to be achievable with the $Ti_3C_2T_x/DNA/PdNp/PtNp$ composite. Using a slightly different approach, Shankar et al.⁵³ combined Ti_2CT_x with graphite composite paste electrodes to detect adrenaline, a catecholamine compound also commonly known as epinephrine. The simultaneous detection of adrenaline, AA and serotonin was achieved using the MXene-containing paste electrode and the limit of detection for adrenaline was determined as 9.5 nM.

Other small molecules, such as glucose and cysteine, which are important in biological systems,⁸¹ have also been electrochemically detected using the titanium carbide MXenes. A three dimensional porous MXene/NiCo-LDH composite was prepared and employed in the non-enzymatic detection of glucose.⁸² Layered double hydroxides (LDH) are generally considered as anionic clay materials, consisting of interlayers of anions, water and positively charged brucite layers.⁸³ The MXene, $Ti_3C_2T_x$, was modified with the NiCo-LDH to form a three dimensional porous network, with the aim of providing a high surface area, with channels for the efficient diffusion of glucose and a conducting MXene substrate for efficient electron transfer. The redox reactions involved in the oxidation of glucose to glucolactone were summarised and these are listed in Equations 5 to 8. The oxidation was observed at 0.45 V vs Ag|AgCl and using chronoamperometry the sensitivity of the sensor was determined as 64.75 $\mu A mM^{-1} cm^{-2}$, with a linear concentration range extending from 2.0 μM to 4.0 mM and a limit of detection of 0.53 μM .



Cysteine, a thiol-containing amino acid, has also been electrochemically detected using a MXene modified glassy carbon electrode.⁸⁴ Palladium nanoparticles, ranging between 2 to 6 nm, were generated at the conducting $Ti_3C_2T_x$ nanoflakes through the in-situ reduction of a Pd(II) salt. The Pd nanoparticles were employed to stabilize the $Ti_3C_2T_x$ nanoflakes in the anodic potential window. In agreement with the study by Lorencova et al.⁷⁴ an irreversible anodic peak appeared at about 430 mV vs Ag|AgCl for the unmodified MXenes and again this was ascribed to the oxidation of $Ti_3C_2T_x$.

The electrochemical detection of these small molecules at $Ti_3C_2T_x$ MXenes and their composites is summarised in Table II. It is clearly evident that impressive detection limits, in the nM concentration range, and very good sensitivities are obtained for several molecules.

MXene-based environmental sensors.—Many organic contaminants, including pesticides and dye molecules, considered as miracle products of the 20th century, are now major environmental contaminants in the 21st century. Furthermore, they are frequently detected in ground and drinking water. For example, Casado et al.⁸⁵ found

Table II. MXene-based sensors for small molecules.

Analyte	Sensor	Sensitivity/ $\mu\text{A mM}^{-1} \text{cm}^{-2}$	LOD/ μM	Ref.
H ₂ O ₂	Ti ₃ C ₂ T _m	-	883	74
H ₂ O ₂	Ti ₃ C ₂ T _m /PtNp	-	0.448	75
H ₂ O ₂	Ti ₃ C ₂ T _m /graphene oxide	-	1.95	76
DA	Ti ₃ C ₂ T _m /Nafion	-	0.003	79
DA	Ti ₃ C ₂ T _m /Pt/Np	3.68	0.26	75
DA	Ti ₃ C ₂ T _m /DNA/PdNp/PtNp	1050	0.030	80
Ep	Ti ₃ C ₂ T _m /GCPE	-	0.0095	53
AA	Ti ₃ C ₂ T _m /Pt/Np	1.41	0.25	75
UA	Ti ₃ C ₂ T _m /Pt/Np	6.85	0.12	75
APAP	Ti ₃ C ₂ T _m /Pt/Np	8.0	0.13	75
Glucose	Ti ₃ C ₂ T _m /NiCo-LDH	-	0.53	82
Cysteine	Ti ₃ C ₂ T _m /PdNp	5.71	0.14	84

Abbreviations: DA, dopamine; Ep, epinephrine (adrenaline); UA, uric acid; APAP, paracetamol; PdNp, palladium nanoparticles; PtNp, platinum nanoparticles; LDH, layered double hydroxides; GCPE, graphite paste electrode.

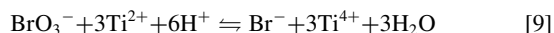
103 different pesticides, with 24 of them being banned on analysing small waterways located in 10 countries in the European Union. Heavy metal ions, such as Cr(VI), Cr(III), As(III) Cu(II), Cd(II) and Ni(II) are also significant contaminants.⁸⁶ There is an increasing demand for the simple and rapid detection of these analytes in water systems and MXenes are attracting considerable attention in environmental applications, primarily as a remediation technology,³⁶⁻³⁸ but also as an electrochemical sensor.

In particular, MXenes have been shown to be very good adsorbents for a number of heavy metal ions.¹³ For example, the complete removal of Ba²⁺ was achieved within 60 min, by using a MXene as a two dimensional adsorbent.⁸⁷ The excellent adsorption properties of MXenes has been attributed to the trapping of cations between the thin interlayer spacing that exists between the MXene nanoflakes. The functional terminal groups on the MXene, and as expected the pH of the analyte solution, also play a significant role. The pH of zero charge has been estimated at a pH of 2.75⁸⁸ indicating that at very acidic conditions, the MXene has a less negative charge and exhibits a lower affinity for the metal cations, but as the pH is increased, the functional groups become ionised providing a negatively charged surface that electrostatically attracts the cations.

This intercalation and adsorption can be exploited in the design of electrochemical sensors, as the adsorption and accumulation of an analyte at a conducting surface can often enhance the electrochemical detection of that analyte. Using this strategy, Zhu et al.⁶¹ modified Ti₃C₂T_x with -OH groups to give an alkylated MXene and used this for the simultaneous electrochemical detection of Cd(II), Pb(II), Cu(II) and Hg(II) using square wave voltammetry. A pre-concentration step was carried out at -1.2 V vs Ag|AgCl for 150 s and then anodic stripping voltammograms were recorded between -1.0 V and 0.5 V vs Ag|AgCl. High sensitivity was achieved with linear ranges between

0.1 μM and 1.0 μM for the four analytes with limits of detection values of 98 nM for Cu(II), 41 nM for Pb(II), 32 nM for Cu²⁺ and 130 nM for Hg(II).

MXenes have also been employed in the electrochemical detection of anionic analytes. For example, a Ti₃C₂T_x-modified glassy carbon electrode was used as the sensor for bromate (BrO₃⁻) and a linear response between 50 nM to 5 μM with a detection limit of 41 nM BrO₃⁻ was achieved.⁶⁰ These studies were carried out in 0.5 M H₂SO₄, facilitating the interaction between the MXene and the negatively charged BrO₃⁻. A broad reduction wave, centred at about -0.55 V vs Ag|AgCl, was attributed to the reduction of BrO₃⁻, Equation 9, and very good selectivity was achieved in the presence of Cl⁻, ClO⁻, NO₃⁻, PO₄⁻ and Br⁻.



Interestingly, the reduction of BrO₃⁻ was not observed at a bare glassy carbon electrode or at a graphene modified electrode. As Equation 9 results in an increase in the oxidation state of titanium, this indicates some changes to the sensing electrode. Using XPS (X-ray photoelectron spectroscopy) TiO₂ crystals were observed following the reduction of BrO₃⁻, consistent with the oxidation of the MXene.

Another approach in the electrochemical detection of environmental contaminants involves the immobilisation of enzymes to give a biosensing platform and this has been employed in the detection of organophosphate pesticides,^{89,90} nitrite⁹¹ and phenol.⁹² One of the most commonly used enzymes in the detection of phosphate-containing pesticides is acetylcholinesterase (AChE), which forms a phosphorylated adduct with the contaminant. As a result, the activity of AChE is inhibited and this decrease in activity can be monitored by measuring the change in the oxidation current of thiocholine (TCh), which is produced from the hydrolysis of

Table III. MXene-based sensors for environmental contaminants.

Analyte	Sensor	Sensitivity/ $\mu\text{A mM}^{-1} \text{cm}^{-2}$	LOD/ μM	Ref.
Cd(II)	Ti ₃ C ₂ T _m (hydroxylated)	7.15	0.098	61
Pb(II)		32.10	0.041	
Cu(II)		20.59	0.032	
Hg(II)		20.47	0.130	
BrO ₃ ⁻	Ti ₃ C ₂ T _m	-	0.041	60
Organophosphates	Ti ₃ C ₂ T _m /AChE/chitosan	-	0.3×10^{-8}	89
Organophosphates	Ti ₃ C ₂ T _m /AChE/MnO ₂ /MnO ₄ /AuNp	-	1.3×10^{-7}	90
nitrite	Ti ₃ C ₂ T _m /Hb	-	0.12	91
phenol	Ti ₃ C ₂ T _m /Tyrosine	414.4	0.012	80

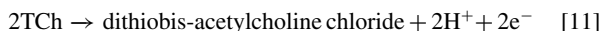
Abbreviations: AuNp, gold nanoparticles; AChE, acetylcholinesterase; Hb, haemoglobin.

Table IV. MXene-based biosensors.

Analyte	Sensor	Sensitivity/ $\mu\text{A mM}^{-1} \text{cm}^{-2}$	LOD/ μM	Ref.
Glucose	$\text{Ti}_3\text{C}_2\text{T}_m/\text{GOx}/\text{AuNp}$	4.2	5.9	97
H_2O_2	$\text{Ti}_3\text{C}_2\text{T}_m/\text{Hb}/\text{Nafion}$	-	0.020	96
H_2O_2	$\text{Ti}_3\text{C}_2\text{T}_m/\text{Hb}/\text{TiO}_2/\text{Nafion}$	447.3	0.014	99
Superoxide anions	$\text{Ti}_3\text{C}_2\text{T}_m/\text{ATP}$	7860	0.5×10^{-3}	100
Carcinoma antigen (CEA)	$\text{Ti}_3\text{C}_2\text{T}_m/\text{APTES}/\text{anti-CEA}/\text{BSA}$	$37.9 \mu\text{A ng}^{-1} \text{mL cm}^{-2}$	$1.8 \times 10^{-5} \text{ ng mL}^{-1}$	101
Gliotoxin	$\text{Ti}_3\text{C}_2\text{T}_m/\text{TDNs}$	-	5×10^{-6}	102
Exosomes	$\text{Ti}_3\text{C}_2\text{T}_m/\text{AuNPs}/\text{PNIPAM}/\text{Apt}$	-	125 particles/ μM	104
Sweat: glucose	$\text{Ti}_3\text{C}_2\text{T}_m/\text{PB composite}$	35.3	0.33	106
Sweat: lactate		11.4	0.67	

Abbreviations: AuNp, gold nanoparticles; Hb, haemoglobin; GOx, glucose oxidase; TDNs, tetrahedral DNA nanostructures; PB, Prussian blue; ATP, adenosine triphosphate; Apt, aptamer; APTES, 3-aminopropyl-triethoxysilane; PNIPAM, Poly(N-isopropylacrylamide), carboxylic acid terminated (PNIPAM, Mn = 2000); BSA, bovine serum albumin.

acetylcholinechloride (ATCl), Equations 10 and 11, to give a sensor. Using this approach AChE was immobilised at a chitosan/ $\text{Ti}_3\text{C}_2\text{T}_x$ composite and used to detect organophosphate pesticides.⁸⁹ More recently, Song et al.⁹⁰ have fabricated a biosensor employing AChE with conducting metal-organic framework-derived $\text{MnO}_2/\text{Mn}_3\text{O}_4$ microcuboids and $\text{Ti}_3\text{C}_2\text{T}_x$ with gold nanoparticles for the detection of methamidophos, an organophosphate pesticide. Using differential pulse voltammetry, the response of the sensor to different pesticide concentrations was followed. A low detection limit of $1.34 \times 10^{-13} \text{ M}$ was achieved, with a broad linear range between 1.0×10^{-12} and $1.0 \times 10^{-6} \text{ M}$ for the detection of the methamidophos.



Other enzymes that have been combined with MXenes are haemoglobin (Hb) and tyrosine. A nitrite sensor was formed by immobilising Hb at $\text{Ti}_3\text{C}_2\text{T}_x$.⁹¹ A broad reduction wave was observed at -0.695 V vs Ag/AgCl and this was attributed to the conversion of nitrite to N_2O . A wide linear range between $0.5 \mu\text{M}$ and 11.8 mM nitrite was obtained with a limit of detection of $0.12 \mu\text{M}$ nitrite. Tyrosinase was immobilised at $\text{Ti}_3\text{C}_2\text{T}_x$ to give a sensor for the sensitive and rapid detection of phenol.⁹² The $\text{Ti}_3\text{C}_2\text{T}_x$ was alkylated to modify the MXene surface with partially terminated $-\text{OH}$ groups, giving a more biocompatible microenvironment for the immobilisation of the enzyme. A rapid response time was achieved and this was attributed to the fast diffusion of phenol from the bulk solution into the immobilised tyrosinase at the MXene nanoflakes coupled with its efficient and fast bioelectrocatalytic reaction. A low detection limit of 12 nM was obtained, with a sensitivity of 414 mA M^{-1} and a linear calibration range between $0.05 \mu\text{M}$ and $15.5 \mu\text{M}$.

The data provided in Table III summarise the applications of MXenes in the detection of various environmental contaminants. Obviously MXenes are promising new materials for the detection of these contaminants and they can be readily combined with enzymes to give sensors for both electroactive and non-electroactive species.

MXene-based biosensors for biomedical applications.—The fabrication of mediator-free electrochemical biosensors, where direct electron transfer (DET) occurs between the enzyme and the electrode, remains challenging as the electroactive redox centre is embedded deep within the protein.^{93–95} Furthermore, a protective microenvironment is needed to retain the activity of the enzyme. Conducting MXenes have the potential to facilitate DET and there is also evidence to suggest that they provide a protective environment for the immobilized enzyme maintaining its bioactivity.⁹⁶ It has been suggested that the enzyme can be easily trapped by the MXene surface groups and as the MXenes have very good charge mobility, electrical communication between the protein and the electrode can be achieved. The MXene-based biosensors used in biomedical applications are summarised in

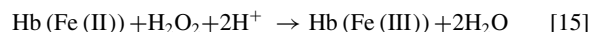
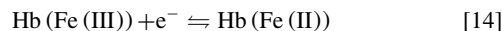
Table IV where it is clearly evident that MXenes are finding applications in the fabrication of biosensors with a number of recent studies and a variety of analytes.

One of the earliest MXene biosensors was designed for the electrochemical detection of glucose. Glucose oxidase (GOx) was immobilised with MXene ($\text{Ti}_3\text{C}_2\text{T}_x$), gold nanoparticles and Nafion at a glassy carbon electrode.⁹⁷ Improved electron transfer, between the redox centre of GOx and the electrode interface, was achieved using the conducting MXene nanoflakes and the gold nanoparticles. This well-known reaction involves the reduction of the Flavin adenine dinucleotide (FAD) through a two electron and two proton transfer reaction to generate FADH_2 , Equation 12.⁹⁸ The FADH_2 is subsequently oxidised back to FAD in the presence of dissolved oxygen generating H_2O_2 , Equation 13.



Nafion was employed not only to act as a membrane to provide selectivity in the presence of AA but it was also employed to disperse the MXenes. The biosensor displayed a high sensitivity of $4.2 \mu\text{A mM}^{-1} \text{cm}^{-2}$, a linear amperometric response in the glucose concentration range of 0.1 to 18 mM and a detection limit of $5.9 \mu\text{M}$.

A mediator-free biosensor for the detection of H_2O_2 has also been reported.^{96,97} In this case, haemoglobin (Hb) was encapsulated using the $\text{Ti}_3\text{C}_2\text{T}_x$ MXene and Nafion was added before the mixture was drop cast onto the electrode.⁹⁶ In a later report TiO_2 nanoparticles were added to increase the surface area available for protein adsorption and to provide a biocompatible microenvironment for the protein.⁹⁹ The catalysed H_2O_2 reduction reaction can be described by Equations 14 and 15.



A well-defined redox couple was observed and this was attributed to the direct electron transfer between the immobilized Hb and the underlying electrode. The H_2O_2 was detected at -0.35 V vs Ag/AgCl using chronoamperometry in a neutral phosphate buffer. The incorporated TiO_2 nanoparticles enhanced the detection of H_2O_2 to give a higher sensitivity and lower detection limit. Using the TiO_2 - $\text{Ti}_3\text{C}_2\text{T}_x$ nanocomposite a wide linear range, extending from $0.1 \mu\text{M}$ to $380 \mu\text{M}$, a sensitivity of $447.3 \mu\text{A mM}^{-1} \text{cm}^{-2}$ and a limit of detection of 14 nM H_2O_2 were achieved. The long-term stability of this sensor was studied and it was found that the biosensor retained 94.6% of its initial response following a 60-day storage period at 4°C . Zheng et al.¹⁰⁰ used adenosine triphosphate (APT) as a template to modify $\text{Ti}_3\text{C}_2\text{T}_x$ with $\text{Mn}_3(\text{PO}_4)_2$ and showed that the conducting MXene enabled the detection of superoxide anions from HepG2 cells.

More recently, $\text{Ti}_3\text{C}_2\text{T}_x$ has been employed in the detection of biomarkers. For example, Kumar et al.¹⁰¹ functionalised $\text{Ti}_3\text{C}_2\text{T}_x$

nanoflakes with (3-aminopropyl)tri-ethoxysilane (APTES) to give $f\text{-Ti}_3\text{C}_2\text{T}_x$. This was then combined with a bio-receptor (anti-CEA) which facilitated the formation of covalent bonds between the amino groups at the $f\text{-Ti}_3\text{C}_2\text{T}_x$ and carboxylic groups from the bio-receptor. Bovine serum albumin (BSA) was added to block unspecific active sites. This sensor was employed for the label free detection of carcinoema bryonic antigen (CEA), a cancer biomarker. The fabricated sensor was used to detect CEA in a phosphate buffer solution with a redox probe, $[\text{Ru}(\text{NH}_3)_6]^{3+}$. Using cyclic voltammetry, the current density was monitored as a function of the CEA concentrations, with a decrease in the current with higher CEA concentrations, indicating specific binding between CEA and the bio-receptor (anti-CEA) and the successful formation of the immune-complex, with a linear detection range of 0.0001 to 2000 ng mL⁻¹. However, a shelf-life study showed a 20% loss in the activity of the sensor over 7 days. $\text{Ti}_3\text{C}_2\text{T}_x$ nanoflakes have also been modified by DNA and used to detect gliotoxin,¹⁰² one of the most toxic metabolites produced during the growth of *Aspergillus fumigatus*.¹⁰³ Tetrahedral DNA nanostructures (TDNs) were immobilised onto the $\text{Ti}_3\text{C}_2\text{T}_x$ nanoflakes, enabled by interactions between the phosphate groups on the DNA and titanium in the MXene. The unique combination of the conducting MXene nanoflakes and configuration of the TDN enabled rapid binding of the gliotoxin to the electrode surface and enhanced electrochemical currents. A particularly low limit of detection, 5 pM, was achieved and linear detection was observed between 5 pM and 10 nM. Interestingly, control studies carried out by replacing the MXene with graphene oxide, GO, and reduced graphene, rGO, showed a much lower current signal for the GO-based sensor. This was explained in terms of the poor conductivity of GO. Although rGO has a much higher conductivity, the loading rate of TDN at the rGO substrate was poor, leading to a low current signal.

Using a similar binding approach, a sensitive electro-generated chemiluminescence (ECL) sensor was developed using aptamer (Apt) modified $\text{Ti}_3\text{C}_2\text{T}_x$ nanoflakes for the detection of exosomes.¹⁰⁴ Exosomes are nanoscale extracellular vesicles that are found in most human bodily fluids and are reported to have an important role in tumor diagnosis.¹⁰⁵ The MXene nanoflakes were employed to increase the loading of the aptamer, to give efficient electron transfer at the electrode interface and also to improve the ECL signal, as the MXenes were found to catalyse the ECL of luminol in the presence of oxygen, without the need for co-reactors, such as H_2O_2 . In this analysis a sandwiched ECL sensor was formed. The $\text{Ti}_3\text{C}_2\text{T}_x$ nanoflakes were modified with an aptamer (Apt2) and used as the nanoprobe electrode (MXenes-Apt2). A second glassy carbon electrode modified with gold nanoparticles was activated in poly(N-isopropylacrylamide) (PNIPAM) and aptamer (Apt1) was immobilised to give GCE/AuNPs-PNIPAM/Apt1. This electrode was exposed to a suspension of exosomes to capture and attach the exosomes to the surface. The sandwiched electrode, MXenes-Apt2/exosomes/Apt1/PNIPAM-AuNPs/GCE, was used in the ECL studies to give a detection limit of 125 particles μL^{-1} , which is over 100 times lower compared to the conventional ELISA method.

MXenes have also been used in the design of wearable sweat-based biosensor patches.¹⁰⁶ In this case, the MXene was combined with Prussian blue (PB) to give a $\text{Ti}_3\text{C}_2\text{T}_x/\text{PB}$ composite that can detect glucose and lactate biomarkers in sweat. A flexible modular biosensing patch was employed with a sweat uptake layer, the sensor layer and a protective cover layer. It was concluded that the 2D morphology and metallic-like conductivity of the MXene gave a distinct improvement in the electrochemical activity, stability and maximised the activity of the enzymes. The MXene system was shown to outperform previously reported graphene/PB and carbon nanotubes/PB based sensors.¹⁰⁶

Stability of MXenes and its impact on MXenes as sensors.—It is clearly evident that MXenes, are promising materials in the fabrication of electrochemical sensors and this is an emerging application area. However, it is now well established that both the multi-layered and single layered nanoflakes of $\text{Ti}_3\text{C}_2\text{T}_x$ gradually degrade in humid air and water environments^{50–52} and this is highly relevant to the

development of MXene-based electrochemical sensors. So far, a number of studies has been reported on the degradation of titanium-based MXenes and especially the Ti_2CT_x and $\text{Ti}_3\text{C}_2\text{T}_x$ MXenes.^{50–52,107–110} It is generally thought that these are gradually transformed into titania, due to hydrolysis reactions with water, and possibly oxidation arising from dissolved oxygen. For example, Zhang et al.⁵² found that open vials of MXene colloidal solutions with water as the solvent degraded by 42%, 85% and 100% after 5, 10 and 15 days, respectively, to give a cloudy white colloidal solution containing TiO_2 . The rate of degradation depended on the size of the nanoflakes with the smaller flakes being the least stable. It was concluded that degradation starts at the flake edges and follows a near exponential decay profile. Huang and Mochalin⁵¹ concluded that it was the presence of water and its hydrolysis reactions that gave rise to the instability of colloidal MXene solutions. They showed that the time constant for the degradation of $\text{Ti}_3\text{C}_2\text{T}_x$ dispersed in anhydrous iso-propanol saturated with pure oxygen, exceeded 5 years, while the same $\text{Ti}_3\text{C}_2\text{T}_x$ dispersion in water was only 41 days. Habib et al.¹⁰⁷ followed the changes in the conductivity of the $\text{Ti}_3\text{C}_2\text{T}_x$ MXenes when exposed to air, liquid, including water, acetonitrile and acetone, and freeze dried as a solid matrix. While oxidation behavior and a loss in conductivity was seen for all conditions, a much slower degradation rate was observed for the solid samples. The authors concluded that the properties of $\text{Ti}_3\text{C}_2\text{T}_x$ MXenes are best maintained in the solid state as powders that can be re-dispersed in the solution phase and to a lesser extent in some organic solvents. They also stated that changes in color and colloidal stability are not always reliable indicators of stability.

In terms of electrochemical sensors, oxidation of $\text{Ti}_3\text{C}_2\text{T}_x$ has been observed at potentials higher than about 0.45 V vs $\text{Ag}|\text{AgCl}$.⁷⁴ However, it appears that by decorating the MXene flakes with metal nanoparticles that this oxidation wave is no longer evident, indicating that the $\text{Ti}_3\text{C}_2\text{T}_x$ MXenes are more stable when combined with metal nanoparticles.⁷⁵ However, it is not clear how these nanoparticles can inhibit the oxidation of the $\text{Ti}_3\text{C}_2\text{T}_x$ flakes and this requires further study. It is also clearly evident that the terminal groups provide ion exchange capacity, or attract cations from the solution phase and this can result in the in-situ reduction of the metal cations. For example, the in-situ reduction of Cu(II) to Cu(I) was observed at $\text{Ti}_3\text{C}_2\text{T}_x$ during the removal of Cu(II) from water,¹¹¹ while Rasheed et al.,⁶⁰ on analysing the surface of $\text{Ti}_3\text{C}_2\text{T}_x$ using X-ray photoelectron spectroscopy (XPS), detected TiO_2 following the in-situ reduction of Pd(II) to generate palladium nanoparticles at the MXene flakes. This is consistent with the partial oxidation of the MXene as the metal ions are reduced and this oxidation process will lead to a loss in the conductivity of the MXene flakes, as they are partially transformed to TiO_2 .

Conclusions and Future Prospects

It is very evident that the titanium carbide MXenes, particularly $\text{Ti}_3\text{C}_2\text{T}_x$, are attractive materials as sensors, with very good conducting properties, high surface areas, excellent hydrophilic properties, they can be easily combined with other materials, easily modified with functional groups, enzymes, proteins and other biomolecules and they appear to provide a protective environment, maintaining the activity of enzymes. They can also be easily decorated with metal nanoparticles and combined with other carbon based materials such as carbon nanotubes and graphene. In many of the published papers where a comparison is made with graphene or carbon nanotubes, the MXenes exhibit higher sensitivities and lower detection limits, out-performing graphene and carbon nanotube based sensors. Nevertheless, they are only emerging now as electrochemical sensors and there is a number of challenges that must be overcome before MXenes can be fully exploited as sensors.

In particular, a long-term evaluation of their biocompatibility, biosafety and biodegradation is required. Although some initial studies have been reported, their long-term toxicity is unknown and their future applications, including sensor development, will depend largely on their biosafety. The stability of MXenes in aqueous environments is another challenge. While these degradation reactions can be

minimised by the selection of suitable organic solvents or by maintaining the MXenes in the solid state, many MXene based sensors will have to function in the presence of water. Again, the long term stability of MXene-based sensors in aqueous solutions is unknown and this requires detailed studies to evaluate the performance of these sensors in aqueous environments and to find ways that can be used to protect MXene sensors from hydrolysis reactions. The current synthetic routes involve HF-etching which raises safety issues and environmental concerns. Moreover, a better understanding of the terminal groups introduced during this etching process is required as these groups and associated defects will have a significant influence on the electron-transfer rate and on the performance of the sensor.

In summary, MXenes have a lot to offer in terms of electrochemical sensors. While only Ti_3C_2Tx , and to a lesser extent Ti_2CTx , has been employed to fabricate sensors, there are a number of other MXenes, including the titanium nitrides, which are predicted to have higher conductivities than the corresponding titanium carbides, making these interesting candidates as sensor materials. However, it is very difficult to selectively etch Al from the titanium nitride MAX phases, presumably because Al is bonded more strongly in the $Ti_{n+1}AlN_n$ and new synthetic approaches are needed to give $Ti_{n+1}N_n$ flakes. Furthermore, as new synthetic approaches are developed, it may be possible to generate the pristine MXenes, without terminal groups. It is known that these terminal groups lower conductivity and the development of a bottom-up-approach that eliminates etching may provide more conducting MXenes. The drop cast methods, commonly used in the fabrication of sensors, give rise to randomly oriented nanoflakes. On the other hand, more control over the orientation of the MXene flakes could possibly enhance their sensing performance, giving higher rates of electron transfer. Finally, in order to further exploit the applications of MXenes, more studies on the chemical functionalisation of MXenes are needed. With the appropriate functionalisation of the surface it could be tailored to bind or form inclusion complexes with specific analytes to give a new highly selective and sensitive sensor platform.

Acknowledgments

This work was supported by the Department of Chemistry at Maynooth University and by Science Foundation Ireland (MTR1261).

ORCID

Carmel B. Breslin  <https://orcid.org/0000-0002-0586-5375>

References

- M. Naguib, M. Kurtoglu, V. Presser, J. Lu, J. Niu, M. Heon, L. Hultman, Y. Gogotsi, and M. W. Barsoum, *Adv. Mater.*, **23**, 4248 (2011).
- Y. Xie, Y. Dall'Agnese, M. Naguib, Y. Gogotsi, M. W. Barsoum, H. L. Zhuang, and P. R. C. Kent, *ACS Nano*, **8**, 9606 (2014).
- Q. Tang, Z. Zhou, and P. Shen, *J. Am. Chem. Soc.*, **134**, 16909 (2012).
- M. Naguib, J. Come, B. Dyatkin, V. Presser, P.-L. Taberna, P. Simon, M. W. Barsoum, and Y. Gogotsi, *Electrochem. Commun.*, **16**, 61 (2012).
- L. Wang, H. Song, L. Yuan, Z. Li, P. Zhang, J. K. Gibson, L. Zheng, H. Wang, Z. Chai, and W. Shi, *Environ. Sci. Technol.*, **53**, 3739 (2019).
- V. M. Hong Ng, H. Huang, K. Zhou, P. S. Lee, W. Que, J. Z. Xu, and L. B. Kong, *J. Mater. Chem. A*, **5**, 3039 (2017).
- Y. Han, Y. Ge, Y. Chao, C. Wang, and G. G. Wallace, *J. Energy Chem.*, **27**, 57 (2018).
- C. Zhang, B. Anasori, A. Seral-Ascaso, S. H. Park, N. McEvoy, A. Shmeliov, G. S. Duesberg, J. N. Coleman, Y. Gogotsi, and V. Nicolosi, *Adv. Mater.*, **29**, 1702678 (2017).
- Z. Guo, J. Zhou, L. Zhu, and Z. Sun, *J. Mater. Chem. A*, **4**, 11446 (2016).
- J. Peng, X. Chen, W. J. Ong, X. Zhao, and N. Li, *Chem.*, **5**, 18 (2019).
- K. Huang, Z. Li, J. Lin, G. Han, and P. Huang, *Chem. Soc. Rev.*, **47**, 5109 (2018).
- H. Lin, Y. Chen, and J. Shi, *Adv. Sci.*, **5**, 1800518 (2018).
- J. Zhu, E. Ha, G. Zhao, Y. Zhou, D. Huang, G. Yue, L. Hu, N. Sun, Y. Wang, L. Y. S. Lee, C. Xu, K.-Y. Wong, D. Astruc, and P. Zhao, *Coord. Chem. Rev.*, **352**, 306 (2017).
- A. Sinha, H. Zhao Dhanjai, Y. Huang, X. Lu, J. Chen, and R. Jain, *Trends Anal. Chem.*, **105**, 424 (2018).
- M. Naguib, V. N. Mochalin, M. W. Barsoum, and Y. Gogotsi, *Adv. Mater.*, **26**, 992 (2014).
- M. R. Lukatskaya, J. Halim, B. Dyatkin, M. Naguib, Y. S. Buranova, M. W. Barsoum, and Y. Gogotsi, *Angew. Chem.*, **53**, 4877 (2014).
- M. W. Barsoum, MAX phases: Properties of machinable ternary carbides and nitrides, Wiley-VCH, Weinheim, 2013.
- M. Alhaheb, K. Maleski, B. Anasori, P. Lelyukh, L. Clark, S. Sin, and Y. Gogotsi, *Chem. Mater.*, **29**, 7633 (2017).
- R. Ma and T. Sasaki, *Acc. Chem. Res.*, **48**, 136 (2015).
- R. M. Ronchi, J. T. Arantes, and S. F. Santos, *Ceram. Int.*, **45**, 18167 (2019).
- M. H. Tran, T. Schaefer, A. Shahraei, M. Duerrschnebel, L. Molina-Luna, U. I. Kramm, and C. S. Birkel, *ACS Appl. Energy Mater.*, **1**, 3908 (2018).
- Y.-W. Cheng, J.-H. Dai, Y.-M. Zhang, and Y. Song, *J. Phys. Chem. C*, **122**, 28113 (2018).
- B. Anasori, Y. Xie, M. Beidaghi, J. Lu, B. C. Hosler, L. Hultman, P. R. C. Kent, Y. Gogotsi, and M. W. Barsoum, *ACS Nano*, **9**, 9507 (2015).
- M. Alhaheb, K. Maleski, T. S. Mathis, A. Sarycheva, C. B. Hatter, S. Uzun, A. Levitt, and Y. Gogotsi, *Angew. Chem. Int. Ed.*, **57**, 5444 (2018).
- A. Lipatov, M. Alhaheb, M. R. Lukatskaya, A. Boson, Y. Gogotsi, and A. Sinitskii, *Adv. Electron. Mater.*, **2**, 1600255 (2016).
- B. Anasori, C. Shi, E. J. Moon, Y. Xie, C. A. Voigt, P. R. C. Kent, S. J. May, S. J. L. Billinge, M. W. Barsoum, and Y. Gogotsi, *Nanoscale Horiz.*, **1**, 227 (2016).
- H. Kim, Z. Wang, and H. N. Alshareef, *Nano Energy*, **60**, 179 (2019).
- A. Qian, J. Y. Seo, H. Shi, J. Y. Lee, and C.-H. Chung, *ChemSusChem*, **11**, 3719 (2018).
- T. Li, L. Yao, Q. Liu, J. Gu, R. Luo, J. Li, X. Yan, W. Wang, P. Liu, B. Chen, W. Zhang, W. Abbas, R. Naz, and D. Zhang, *Angew. Chem. Int. Ed.*, **57**, 6115 (2018).
- C. Dai, H. Lin, G. Xu, Z. Liu, R. Wu, and Y. Chen, *Chem. Mater.*, **29**, 8637 (2017).
- F. Shahzad, M. Alhaheb, C. B. Hatter, B. Anasori, S. M. Hong, C. M. Koo, and Y. Gogotsi, *Science*, **353**, 1137 (2016).
- I. R. Shein and A. L. Ivanovskii, *Comput. Mater. Sci.*, **65**, 104 (2012).
- M. Malaki, A. Maleki, and R. S. Varma, *J. Mater. Chem. A*, **7**, 10843 (2019).
- L. Verger, C. Xu, V. Natu, H.-M. Cheng, W. Ren, and M. W. Barsoum, *Curr. Opin. Solid State Mater. Sci.*, **23**, 149 (2019).
- Y. Zhang, N. Zhang, and C. Ge, *Mater.*, **11**, 2281 (2018).
- B.-M. Jun, S. Kim, J. Heo, C. M. Park, N. Her, M. Jang, Y. Huang, J. Han, and Y. Yoon, *Nano Res.*, **12**, 471 (2019).
- Y. Zhang, L. Wang, N. Zhang, and Z. Zhou, *RSC Adv.*, **8**, 19895 (2018).
- Y. Wu, H. Pang, Y. Liu, X. Wang, S. Yu, D. Fu, J. Chen, and X. Wang, *Environ. Pollut.*, **246**, 608 (2019).
- X. Chia and M. Pumera, *Nat. Catal.*, **1**, 909 (2018).
- Z. Li, Z. Qi, S. Wang, T. Ma, L. Zhou, Z. Wu, X. Luan, F.-Y. Lin, M. Chen, J. T. Miller, J. Xin, W. Huang, and Y. Wu, *Nano Lett.*, **19**, 5102 (2019).
- G. Li, Y. Xia, Y. Tian, Y. Wu, J. Liu, Q. He, and D. Chen, *J. Electrochem. Soc.*, **166**, B881 (2019).
- H. Razmi, L. Ezzati, and Z. Khorablou, *J. Electrochem. Soc.*, **166**, B961 (2019).
- K. Samoson, P. Thavarungkul, P. Kanatharana, and W. Limbut, *J. Electrochem. Soc.*, **166**, B1079 (2019).
- N. M. M. A. Edris, J. Abdullah, S. Kamaruzaman, and Y. Sulaiman, *J. Electrochem. Soc.*, **166**, B664 (2019).
- M. Ghidui, M. R. Lukatskaya, M. Q. Zhao, Y. Gogotsi, and M. W. Barsoum, *Nature*, **516**, 78 (2014).
- X. Sang, Y. Xie, M.-W. Lin, M. Alhaheb, K. L. Van Aken, Y. Gogotsi, P. R. C. Kent, K. Xiao, and R. R. Unocic, *ACS Nano*, **10**, 9193 (2016).
- W. Sun, S. A. Shah, Y. Chen, Z. Tan, H. Gao, T. Habib, M. Radovic, and M. J. Green, *J. Mater. Chem. A*, **5**, 21663 (2017).
- S.-Y. Pang, Y.-T. Wong, S. Yuan, Y. Liu, M.-K. Tsang, Z. Yang, H. Huang, W.-T. Wong, and J. Hao, *J. Am. Chem. Soc.*, **141**, 9610 (2019).
- S. Yang, P. Zhang, F. Wang, A. G. Ricciardulli, M. R. Lohe, P. W. M. Blom, and X. Feng, *Angew. Chem. Int. Ed.*, **57**, 15491 (2018).
- I.-M. Low, *Mater.*, **12**, 473 (2019).
- S. Huang and V. N. Mochalin, *Inorg. Chem.*, **58**, 1958 (2019).
- C. Zhang, S. Pinilla, N. McEvoy, C. P. Cullen, B. Anasori, E. Long, S.-H. Park, A. Seral-Ascaso, A. Shmeliov, D. Krishnan, C. Morant, X. Liu, G. S. Duesberg, Y. Gogotsi, and V. Nicolosi, *Chem. Mater.*, **29**, 4848 (2017).
- S. S. Shankar, R. M. Shereema, and R. B. Rakhi, *ACS Appl. Mater. Interfaces*, **10**, 43343 (2018).
- M. R. Nateghi, *Russ. J. Electrochem.*, **55**, 52 (2019).
- M. Rizk, E. A. Taha, M. M. A. Abou El-Alamin, H. A. M. Hendawy, and Y. M. Sayed, *J. Electrochem. Soc.*, **165**, H333 (2018).
- Z. Pourghobadi and R. Pourghobadi, *J. Electrochem. Soc.*, **166**, B76 (2019).
- T. Gurusamy, A. Banerjee, N. Chandrakumar, and K. Ramanujam, *J. Electrochem. Soc.*, **166**, B1186 (2019).
- S. Rodsud and W. Limbut, *J. Electrochem. Soc.*, **166**, B771 (2019).
- Z. Chen, Y. Zhang, J. Zhang, and J. Zhou, *J. Electrochem. Soc.*, **166**, B787 (2019).
- P. Abdul Rasheed, R. P. Pandey, K. Rasool, and K. A. Mahmoud, *Sens. Actuators, B*, **265**, 652 (2018).
- X. Zhu, B. Liu, H. Hou, Z. Huang, K. M. Zeinu, L. Huang, X. Yuan, D. Guo, J. Hu, and J. Yang, *Electrochim. Acta*, **248**, 46 (2017).
- M. Vural, A. Pena-Francesch, J. Bars-Pomes, H. Jung, H. Gudapati, C. B. Hatter, B. D. Allen, B. Anasori, I. T. Ozbolat, Y. Gogotsi, and M. C. Demirel, *Adv. Funct. Mater.*, **28**, 1801972 (2018).
- H. Hu and T. Hua, *J. Mater. Chem. A*, **5**, 19639 (2017).
- M. Mariano, O. Mashtalir, F. Q. Antonio, W.-H. Ryu, B. Deng, F. Xia, Y. Gogotsi, and A. D. Taylor, *Nanoscale*, **8**, 16371 (2016).
- X. Wu, B. Huang, R. Lv, Q. Wang, and Y. Wang, *Chem. Eng. J.*, **378**, 122246 (2019).
- L. Chen, Y. Lin, J. Fu, J. Xie, R. Chen, and H. Zhang, *ChemElectroChem*, **5**, 3307 (2018).
- P. Liu, V. M. H. Ng, Z. Yao, J. Zhou, and L. B. Kong, *Mater. Lett.*, **229**, 286 (2018).

68. I. Demiroglu, F. M. Peeters, O. Gülsiren, D. Çakır, and C. Sevik, *J. Phys. Chem. Lett.*, **10**, 727 (2019).
69. S. Xu, Y. Dall'Agnese, J. Li, Y. Gogotsi, and W. Han, *Chem. Eur. J.*, **24**, 18556 (2018).
70. J. Chen, X. Yuan, F. Lyu, Q. Zhong, H. Hu, Q. Pan, and Q. Zhang, *J. Mater. Chem.*, **7**, 1281 (2019).
71. Y. Li, G. Ran, W. J. Yi, H. Q. Luo, and N. B. Li, *Microchim. Acta*, **178**, 115 (2012).
72. C. C. Harley, A. D. Rooney, and C. B. Breslin, *Sens. Actuators, B*, **150**, 498 (2010).
73. R. Jerome and A. K. Sundramoorthy, *J. Electrochem. Soc.*, **166**, B3017 (2019).
74. L. Lorencova, T. Bertok, E. Dosekova, A. Holazova, D. Paprkova, A. Vikartovska, V. Sasinkova, J. Filip, P. Kasak, M. Jerigova, D. Velic, K. A. Mahmoud, and J. Tkac, *Electrochim. Acta*, **235**, 471 (2017).
75. L. Lorencova, T. Bertok, J. Filip, M. Jerigova, D. Velic, P. Kasak, K. A. Mahmoud, and J. Tkac, *Sens. Actuators, B*, **263**, 360 (2018).
76. J. Zheng, J. Diao, Y. Jin, A. Ding, B. Wang, L. Wu, B. Weng, and J. Chen, *J. Electrochem. Soc.*, **165**, B227 (2018).
77. J. Lu, L. T. Drzal, R. M. Worden, and I. Lee, *Chem. Mater.*, **19**, 6240 (2007).
78. X.-M. Miao, R. Yuan, Y.-Q. Chai, Y.-T. Shi, and Y.-Y. Yuan, *J. Electroanal. Chem.*, **612**, 157 (2008).
79. F. Shahzad, A. Iqbal, S. A. Zaidi, S.-W. Hwang, and C. M. Koo, *J. Ind. Eng. Chem.*, (2019).
80. J. Zheng, B. Wang, A. Ding, B. Weng, and J. Chen, *J. Electroanal. Chem.*, **816**, 189 (2018).
81. J. D. Newman and A. P. F. Turner, *Biosens. Bioelectron.*, **20**, 2435 (2005).
82. M. Li, L. Fang, H. Zhou, F. Wu, Y. Lu, H. Luo, Y. Zhang, and B. Hu, *Appl. Surf. Sci.*, **495**, 143554 (2019).
83. B. Hai and Y. Zou, *Sens. Actuators, B*, **208**, 143 (2015).
84. P. A. Rasheed, R. P. Pandey, K. A. Jabbar, J. Ponraj, and K. A. Mahmoud, *Anal. Meth.*, **11**, 3851 (2019).
85. J. Casado, K. Brigden, D. Santillo, and P. Johnston, *Sci. Total Environ.*, **670**, 1204 (2019).
86. X. Guo and F. Chen, *Environ. Sci. Technol.*, **39**, 6808 (2005).
87. A. K. Fard, G. McKay, R. Chamoun, T. Rhadfi, H. Preud'Homme, and M. A. Atieh, *Chem. Eng. J.*, **317**, 331 (2017).
88. L. Wang, H. Song, L. Yuan, Z. Li, Y. Zhang, J. K. Gibson, L. Zheng, Z. Chai, and W. Shi, *Environ. Sci. Technol.*, **52**, 10748 (2018).
89. L. Zhou, X. Zhang, L. Ma, J. Gao, and Y. Jiang, *Biochem. Engineering J.*, **128**, 243 (2017).
90. D. Song, X. Jiang, Y. Li, X. Lu, S. Luan, Y. Wang, Y. Li, and F. Gao, *J. Hazard. Mater.*, **373**, 367 (2019).
91. H. Liu, C. Duan, C. Yang, W. Shen, F. Wang, and Z. Zhu, *Sens. Actuators, B*, **218**, 60 (2015).
92. L. Wu, X. Lu, Z. S. Wu Dhanjai, Y. Dong, X. Wang, S. Zheng, and J. Chen, *Biosens. Bioelectron.*, **107**, 69 (2018).
93. M. Wooten, S. Karra, M. Zhang, and W. Gorski, *Anal. Chem.*, **86**, 752 (2014).
94. L. Xiao, Y. Ding, Q. Zhai, M. Hu, S. Li, Y. Wang, Y. Chen, and Y. Jiang, *J. Electrochem. Soc.*, **166**, G67 (2019).
95. T. Nöll and G. Nöll, *Chem. Soc. Rev.*, **40**, 3564 (2011).
96. F. Wang, C. H. Yang, C. Y. Duan, D. Xiao, Y. Tang, and J. F. Zhu, *J. Electrochem. Soc.*, **162**, B16 (2015).
97. R. B. Rakhi, P. Nayak, C. Xia, and H. N. Alshareef, *Scientific Rep.*, **6**, 36422 (2016).
98. R. Wilson and A. P. F. Turner, *Biosens. Bioelectron.*, **7**, 165 (1992).
99. F. Wang, C. Yang, M. Duan, Y. Tang, and J. F. Zhu, *Biosens. Bioelectron.*, **74**, 1022 (2015).
100. J. Zheng, B. Wang, Y. Jin, B. Weng, and J. Chen, *Microchim. Acta*, **186**, 95 (2019).
101. S. Kumar, Y. Lei, N. H. Alshareef, M. A. Quevedo-Lopez, and K. N. Salama, *Biosens. Bioelectron.*, **121**, 243 (2018).
102. H. Wang, H. Li, Y. Huang, M. Xiong, F. Wang, and C. Li, *Biosens. Bioelectron.*, **142**, 111531 (2019).
103. T. R. T. Dagenais and N. P. Keller, *Clin. Microbiol. Rev.*, **22**, 447 (2009).
104. H. Zhang, Z. Wang, Q. Zhang, F. Wang, and Y. Liu, *Biosens. Bioelectron.*, **124**, 184 (2019).
105. C. Théry, L. Zitvogel, and S. Amigorena, *Nat. Rev. Immunol.*, **2**, 569 (2002).
106. Y. Lei, W. Zhao, Y. Zhang, Q. Jiang, J.-H. He, A. J. Baeumner, O. S. Wolfbeis, Z. L. Wang, K. N. Salama, and H. N. Alshareef, *Small*, **15**, 1901190 (2019).
107. T. Habib, X. Zhao, S. A. Shah, Y. Chen, W. Sun, H. An, J. L. Lutkenhaus, M. Radovic, and M. J. Green, *npj 2D Mater. Appl.*, **3**, 8 (2019).
108. Y. Chae, S. J. Kim, S.-Y. Cho, J. Choi, K. Maleski, B.-J. Lee, H.-T. Jung, Y. Gogotsi, Y. Lee, and C. W. Ahn, *Nanoscale*, **11**, 8387 (2019).
109. R. Thakur, A. VahidMohammadi, J. Moncada, W. R. Adams, M. Chi, B. Tatarчук, M. Beidaghi, and C. A. Carrero, *Nanoscale*, **11**, 10716 (2019).
110. A. Rozmyslowska, T. Wojciechowski, W. Ziembowska, L. Chlubny, A. Olszyna, S. Pozniak, K. Tomkiewicz, and A. M. Jastrzebska, *Int. J. Electrochem. Sci.*, **13**, 10837 (2018).
111. A. Shahzad, K. Rasool, W. Miran, M. Nawaz, J. Jang, K. A. Mahmoud, and D. S. Lee, *ACS Sustainable Chem. Eng.*, **5**, 11481 (2017).